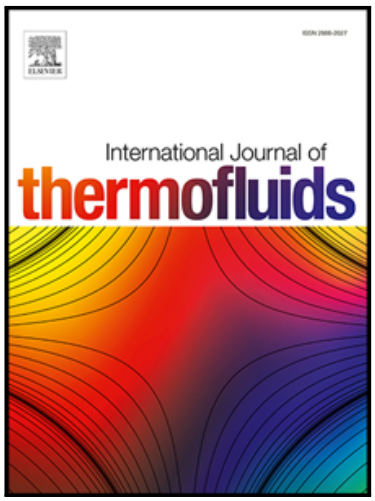

Simultaneous estimation of heat flux and heat transfer coefficient in irregular geometries made of functionally graded materials

Farzad Mohebbi , Ben Evans

PII: S2666-2027(19)30009-6
DOI: https://doi.org/10.1016/j.ijft.2019.100009
Reference: IJTF 100009

To appear in: *International Journal of Thermofluids*

Received date: 31 October 2019
Revised date: 22 December 2019
Accepted date: 22 December 2019

Please cite this article as: Farzad Mohebbi , Ben Evans , Simultaneous estimation of heat flux and heat transfer coefficient in irregular geometries made of functionally graded materials, *International Journal of Thermofluids* (2020), doi: https://doi.org/10.1016/j.ijft.2019.100009

Simultaneous estimation of heat flux and heat transfer coefficient in irregular geometries made of functionally graded materials

Farzad Mohebbi*, Ben Evans

Zienkiewicz Centre for Computational Engineering, College of Engineering, Swansea

University, Bay Campus, Fabian Way, Crymlyn Burrows, Swansea SA1 8EN, UK

Abstract. A numerical inverse analysis based on explicit sensitivity coefficients is developed for the simultaneous estimation of heat flux and heat transfer coefficient imposed on different parts of boundary of a general irregular heat conducting body made of functionally graded materials with spatially varying thermal conductivity. It is assumed that the thermal conductivity varies exponentially with position in the body. The body considered in this study is an eccentric hollow cylinder. The heat flux is applied on the cylinder inner surface and the heat is dissipated to the surroundings through the outer surface. The numerical method used in this study consists of three steps: 1) to apply a boundary-fitted grid generation (elliptic) method to generate grid over eccentric hollow cylinder (an irregular shape) and then solve for the steady-state heat conduction equation with variable thermal conductivity to compute the temperature values in the cylinder, 2) to propose a new explicit sensitivity analysis scheme used in inverse analysis, and 3) to apply a gradient-based optimization method (in this study, conjugate gradient method) to minimize the mismatch between the computed temperature on the outer surface of the cylinder and simulated measured temperature distribution. The inverse analysis presented here is not involved with an adjoint equation and all the sensitivity coefficients can be computed in only one direct solution, without the need for the solution of the adjoint equation. The accuracy, efficiency, and robustness of the developed inverse analysis are demonstrated through presenting a test case with different initial guesses.

Keywords:

Inverse Heat Transfer Problems; Functionally Graded Materials; Spatially varying thermal conductivity; Explicit sensitivity analysis; Finite-difference method; Conjugate gradient method

1. Introduction

Direct heat transfer problems deal with the determination of temperature distribution in a heat conducting body from the known boundary conditions, the thermo-physical properties, and the geometric configuration of the heat conducting body. Unlike the direct heat transfer problems, inverse heat transfer problems (IHTPs) are concerned with the determination of

* Corresponding author
Email address: farzad.mohebbi@swansea.ac.uk, farzadmohebbi@yahoo.com

the boundary conditions, the thermo-physical properties, and the geometric configuration of the heat conducting body from the temperature measurement taken at some points inside the body or on some part of the boundary. The temperature distribution over heat conducting bodies can be obtained accurately as long as the thermo-physical properties and the associated boundary conditions are precisely known. However, accurate knowledge of these parameters relies on conducting expensive experiments with sophisticated instruments. These parameters may be estimated in an inexpensive manner using inverse methods. Over the past decades, inverse analysis has been extensively used to determine the thermal conductivity (constant, temperature-dependent, and spatially varying parameter) and the convection heat transfer coefficient [1-31] , the heat flux [32-34], and the boundary shape of bodies [35-39] using temperature measurement taken at some points inside the body or on some part of the boundary. However, the inverse heat transfer problems are ill-posed and mathematically challenging because the ill-posed problems are inherently unstable and very sensitive to small errors in input data. With the advent of high-speed computers, different numerical methods have been developed to deal with the inverse heat transfer problems and their ill-posed nature and overcome the instabilities of these problems. Among such numerical methods are iterative regularization techniques in which the solution of the inverse problem is improved sequentially. In these iterative methods, the discrepancy principle may be used as a criterion to stop the iteration and obtain a reasonably stable solution [40, 41].

Functionally graded materials (FGMs), a relatively new class of composite materials, are inhomogeneous composites which are composed of two or more constituents phases [42-44]. These materials have extensive applications in extremely high temperature environments such as nuclear reactors, pressure vessel, and chemical plants [45]. The properties of these materials (such as thermal conductivity, modulus of elasticity, density, etc) vary smoothly and continuously with position by gradually varying the volume fraction of constituent materials [42]. Exponential type is one of commonly used material graduation forms for considering the variation of thermal conductivity of the functionally graded materials with position. In addition to the stress analysis, the direct and inverse heat transfer analysis of functionally graded hollow cylinders has also received much attention due to extensive use of them in industry [46-49]. In [46], an inverse transient heat conduction analysis is presented to estimate the imposed heat flux or the convective heat transfer coefficient on the inner surface of a long multi-layered functionally graded cylinder using the measured temperature on the outer surface of the cylinder. In [47], the unknown space-dependent thermal conductivity of a functionally graded hollow cylinder is estimated using an inverse analysis. The conjugate gradient method and the discrepancy principle were employed and the success of the inverse method depends on the type of the boundary conditions. In [48], an analytical method is used to study the transient heat conduction in a cylindrical shell of functionally graded material. It is assumed that the thermal conductivity is the power function of the radius of the cylinder. In [49], an inverse analysis based on the conjugate gradient method is used to estimate the time-dependent heat flux at the inner surface of a functionally graded hollow cylinder by using the simulated temperature measurements taken within the cylinder.

However, analytical and numerical solutions of the direct and inverse heat conduction problems in the functionally graded hollow cylinders include limitations such as one-dimensional (radial) analysis only, complexity of numerical method, significant implementation efforts, inability to considering a variety of boundary conditions, solution of

additional equations such as adjoint equation, high computational cost, separate estimation, and accuracy. So an accurate, efficient, and easy to implement method to handle the direct and the inverse heat conduction problems with an ability to consider the Dirichlet, the Neumann, and the Robin boundary condition to estimate the unknown parameters separately and simultaneously may be required. The estimation of the unknown parameters simultaneously has the advantage that two or more parameters involved in heat transfer problems may be estimated more efficient than when the parameters are estimated separately due to the number of the direct problem solutions. Moreover, due to the importance of eccentricity in heat transfer analysis of hollow cylinders [50, 51], in this study, an eccentricity is added to the functionally graded hollow cylinder problem to reveal the applicability of the proposed method to the geometries including eccentricity (an irregular geometry). In other words, the proposed method can be equally applied to the direct and the inverse heat conduction problems in the functionally graded hollow cylinders with and without eccentricity.

To our knowledge, simultaneous estimation of boundary conditions imposed on different parts of boundary of FGMs (heat conducting bodies with spatially varying thermal conductivity) with an irregular shape using an inverse heat transfer analysis has not been investigated as yet. In this study, a numerical inverse analysis based on a new explicit sensitivity analysis scheme is developed for the simultaneous estimation of applied heat flux and heat transfer coefficient in a functionally graded eccentric hollow cylinder with spatially varying thermal conductivity. The thermal conductivity is assumed to vary exponentially with position in the cylinder. The heat flux is applied on the cylinder inner surface and the heat is dissipated to the surroundings through the outer surface. The elliptic grid generation technique is used to generate a mesh over the irregular body and then solve for the steady-state heat conduction equation by transforming the cylinder shape (physical domain), the governing equation and the associated boundary conditions onto the computational domain. The discretization in the computational domain is carried out by the finite-difference method, a method chosen for its simplicity and ease of implementation. The novel aspect of the inverse analysis is its very efficient and accurate sensitivity analysis scheme in which explicit and easy to implement expressions for the sensitivity coefficients are derived which allow for the efficient and accurate computation of all sensitivity coefficients in one single direct problem solution only without the need for the solution of adjoint equation. The conjugate gradient method is used to minimize the objective function which is the difference between the computed temperature on part of the boundary and the measured temperature.

The gradient of the objective function with respect to the unknown variables (here the heat flux and the heat transfer coefficient) can be computed using the solution of the adjoint method. In addition to the mathematical complexity, the computational cost of the solution of the adjoint equation is comparable to the solution of the direct heat conduction equation. Hence, the total computational cost of the computation of the gradient of the objective function with respect to the variables is roughly equal to the computational cost of two direct heat conduction equation solution at each iteration. As an alternative, if the finite-difference method is used to compute the sensitivity of the objective function to the variables, two (number of variables here) additional solutions of the direct heat conduction equation are needed which means a computational cost of three solutions of the direct heat conduction equation at each iteration. As already mentioned, the explicit sensitivity coefficients derived in

this study allow for the computation of all sensitivity coefficients with a negligible computational cost thereby computing the gradient of the objective function in one single direct heat conduction equation solution only without the need for the solution of adjoint equation or additional solutions of the direct problem. As the inverse analysis used in this study involves a large number of iterations to recover the unknown variables, the use of the proposed sensitivity analysis scheme decreases the computational cost significantly (due to less computational cost at each iteration). As will be shown, the sensitivity analysis scheme is also accurate and robust. Moreover, as the heat flux is applied at the inner surface of the hollow cylinder and the temperature measurements are taken on the outer surface (a different surface from the applied heat flux surface), one needs to relate the measured temperatures to the heat flux conveniently. As will be shown, the chain rule using the variable thermal conductivity components may be used to obtain such a relation.

It should be noted that the although the cylinder inner and outer surface shapes are regular (circular), the eccentric hollow cylinder shape is irregular. Moreover, the formulations developed in this study to solve direct and inverse problems are *general* and can also be used for irregular inner and outer surface shapes as long as the general body shape can be mapped onto regular computational domain.

2. Governing equation

The heat conducting body (eccentric hollow cylinder) shown in Fig. 1 is made of functionally graded materials in which thermal conductivity varies exponentially with position in the cylinder. In other words, $k = a_1 e^{(1+a_2 x)} e^{(1+a_3 y)}$. For this problem, the two-dimensional steady-state heat conduction equation with no heat generation can be stated as below

$$\frac{\partial}{\partial x}(k(x,y)\frac{\partial T}{\partial x}) + \frac{\partial}{\partial y}(k(x,y)\frac{\partial T}{\partial y}) = 0 \quad \text{in physical domain } \Omega \tag{1}$$

subject to the boundary conditions

$$\frac{\partial T}{\partial n_i} = \frac{\dot{q}}{k} \text{ on (inner) boundary surface } \Gamma_i \tag{2}$$

$$\frac{\partial T}{\partial n_o} = -\frac{h}{k}(T_{\Gamma_o} - T_\infty) \text{ on (outer) boundary surface } \Gamma_o \tag{3}$$

where $k(x,y)$ is the thermal conductivity which varies exponentially over the domain Ω.

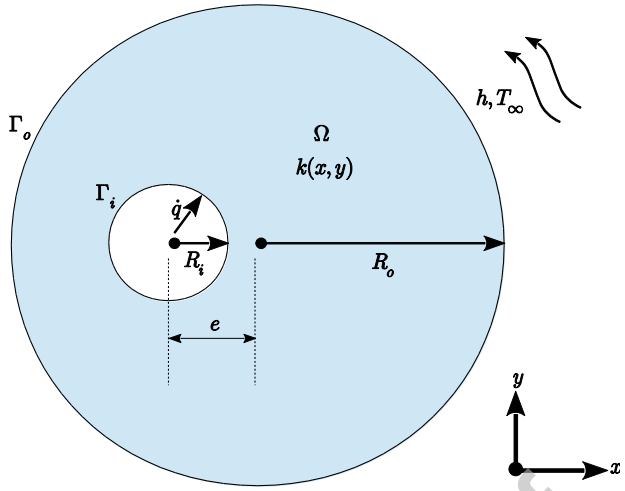

Fig. 1 Eccentric hollow cylinder made of functionally graded materials is subjected to convective heat transfer on outer surface and heat flux $\dot{q}$ on inner surface. The thermal conductivity $k(x,y)$ varies exponentially with position in the cylinder.

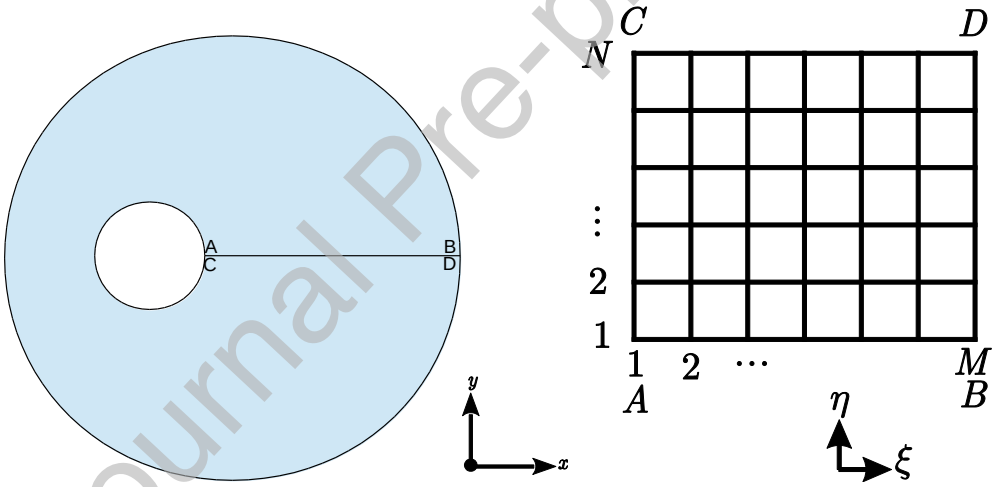

a) b)

Fig. 2. Eccentric hollow cylinder (the physical domain) (a) and the corresponding computational domain (b).

Here as the body shape is irregular, the elliptic grid generation method is used to discretize the physical domain and then the finite-difference method is used to approximate the derivatives of the field variable (temperature) at grid nodes by algebraic ones. This method is based on mapping the irregular physical domain (Fig. 2a) from the x and y physical plane onto the ξ and η computational one (Fig. 2b). Then the heat conduction equation and the associated boundary conditions (Eqs.(1) to (3)) are transformed from the x and y physical plane to the ξ and η computational plane. More details on the implementation of the elliptic

grid generation technique and solution procedure for the steady-state heat conduction equation can be found in [52]. Since the thermal conductivity is not constant and is a spatially varying parameter, we can expand Eq. (1) as follows

$$\frac{\partial k}{\partial x}\frac{\partial T}{\partial x}+k\frac{\partial^2 T}{\partial x^2}+\frac{\partial k}{\partial y}\frac{\partial T}{\partial y}+k\frac{\partial^2 T}{\partial y^2}=0$$

by simplifying, we get

$$k(\frac{\partial^2 T}{\partial x^2}+\frac{\partial^2 T}{\partial y^2})+\frac{\partial k}{\partial x}\frac{\partial T}{\partial x}+\frac{\partial k}{\partial y}\frac{\partial T}{\partial y}=0 \tag{4}$$

for the exponential material graduation type

$$k=a_1e^{(1+a_2x)}e^{(1+a_3y)} \tag{5}$$

$$k_x=\frac{\partial k}{\partial x}=a_2a_1e^{(1+a_2x)}e^{(1+a_3y)} \tag{6}$$

$$k_y=\frac{\partial k}{\partial y}=a_3a_1e^{(1+a_2x)}e^{(1+a_3y)} \tag{7}$$

Thus Eq. (4) becomes

$$a_1e^{(1+a_2x)}e^{(1+a_3y)}(\frac{\partial^2 T}{\partial x^2}+\frac{\partial^2 T}{\partial y^2})+a_2a_1e^{(1+a_2x)}e^{(1+a_3y)}\frac{\partial T}{\partial x}+a_3a_1e^{(1+a_2x)}e^{(1+a_3y)}\frac{\partial T}{\partial y}=0 \tag{8}$$

or

$$a_1e^{(1+a_2x)}e^{(1+a_3y)}\left[(\frac{\partial^2 T}{\partial x^2}+\frac{\partial^2 T}{\partial y^2})+a_2\frac{\partial T}{\partial x}+a_3\frac{\partial T}{\partial y}\right]=0 \tag{9}$$

Since $k=a_1e^{(1+a_2x)}e^{(1+a_3y)}\neq 0$, we get

$$(\frac{\partial^2 T}{\partial x^2}+\frac{\partial^2 T}{\partial y^2})+a_2\frac{\partial T}{\partial x}+a_3\frac{\partial T}{\partial y}=0 \tag{10}$$

by substituting for T_x, T_y, T_{xx}, and T_{yy} using the transformation relationships and the finite-difference expressions [52], Eq. (4) will be

$$\left[\frac{1}{J^2}(\alpha T_{\xi\xi}-2\beta T_{\xi\eta}+\gamma T_{\eta\eta})\right]+a_2\left[\frac{1}{J}(y_\eta T_\xi-y_\xi T_\eta)\right]+a_3\left[\frac{1}{J}(-x_\eta T_\xi+x_\xi T_\eta)\right]=0 \tag{11}$$

where

$$f_{\xi} = \frac{1}{2}(f_{i+1,j} - f_{i-1,j})$$

$$f_{\eta} = \frac{1}{2}(f_{i,j+1} - f_{i,j-1})$$

$$f_{\xi\xi} = f_{i+1,j} - 2f_{i,j} + f_{i-1,j}$$

$$f_{\eta\eta} = f_{i,j+1} - 2f_{i,j} + f_{i,j-1}$$

$$f_{\xi\eta} = \frac{1}{4}(f_{i+1,j+1} - f_{i-1,j+1} - f_{i+1,j-1} + f_{i-1,j-1}) \tag{12}$$

where $f \equiv x, y, T$. And

$$\alpha = x_{\eta}^2 + y_{\eta}^2$$

$$\beta = x_{\xi}x_{\eta} + y_{\xi}y_{\eta}$$

$$\gamma = x_{\xi}^2 + y_{\xi}^2$$

$$J = x_{\xi}y_{\eta} - x_{\eta}y_{\xi} \qquad \text{Jacobian of transformation} \tag{13}$$

are the coefficients obtained from the elliptic grid generation method. By knowing the values for a_l, $l = 1,2,3$ as well as $x_{i,j}$ and $y_{i,j}$ (nodal coordinates) from the elliptic grid generation step, Eq. (11) may be solved using an algebraic solver such as Maple to obtain an expression for $T_{i,j}$ in the body, as follows

$$T_{i,j} = \frac{-0.5}{(\alpha+\gamma)}(-\alpha T_{i+1,j} - \alpha T_{i-1,j} + 2\beta T_{\xi\eta} - \gamma T_{i,j+1} - \gamma T_{i,j-1} - a_2 J y_{\eta} T_{\xi} + a_2 J y_{\xi} T_{\eta} + a_3 J x_{\eta} T_{\xi} - a_3 J x_{\xi} T_{\eta}) \tag{14}$$

The term $\frac{\partial T}{\partial n}$ at a boundary surface in the physical domain is related to $\frac{\partial T}{\partial \xi}$ and/or $\frac{\partial T}{\partial \eta}$ at the corresponding transformed boundary surface in the computational domain. At the inner surface Γ_i and the outer surface Γ_o, we have [52]

$$\text{at inner surface } \Gamma_i : \frac{\partial T}{\partial n_i} = \frac{-1}{J\sqrt{\alpha}}(\alpha T_{\xi} - \beta T_{\eta}) \tag{15}$$

$$\text{at outer surface } \Gamma_o : \frac{\partial T}{\partial n_o} = \frac{1}{J\sqrt{\alpha}}(\alpha T_\xi - \beta T_\eta) \tag{16}$$

Thus, the boundary condition equation at the outer surface Γ_o for the exponential material graduation type is written as

$$\dot{q}_{\text{conduction}} \,|_{\Gamma_o} = \dot{q}_{\text{convection}} \,|_{\Gamma_o} \tag{17}$$

$$-k\frac{\partial T}{\partial n_o} = h(T_{\Gamma_o} - T_\infty) \tag{18}$$

$$-k\left[\frac{1}{J\sqrt{\alpha}}(\alpha T_\xi - \beta T_\eta)\right] = h(T_{\Gamma_o} - T_\infty) \tag{19}$$

at the outer surface Γ_o, we have

$$T_\xi = \frac{1}{2}(3T_{M,j} - 4T_{M-1,j} + T_{M-2,j}) \tag{20}$$

$$T_\eta = \frac{1}{2}(T_{M,j+1} - T_{M,j-1}) \tag{21}$$

Therefore, Eq. (19) becomes

$$-k_{M,j}\left[\frac{1}{J\sqrt{\alpha}}\left(\alpha\frac{3T_{M,j} - 4T_{M-1,j} + T_{M-2,j}}{2} - \beta\frac{T_{M,j+1} - T_{M,j-1}}{2}\right)\right] = h\ T_{M,j} - T_\infty \tag{22}$$

where the coefficients J, γ, and β defined in Eq. (13) are computed using the finite-difference coefficients associated with the outer surface Γ_o. Solving Eq. (22) for $T_{M,j}$ gives the temperature distribution on the boundary surface Γ_o as follows

$$T_{M,j} = \frac{k_{M,j}(4\alpha T_{M-1,j} - \alpha T_{M-2,j} + \beta T_{M,j+1} - \beta T_{M,j-1}) + 2hJ\sqrt{\alpha}T_\infty}{3k_{M,j}\alpha + 2hJ\sqrt{\alpha}} \tag{23}$$

or

$$T_{M,j} = \frac{a_1 e^{(1+a_2 x_{M,j})} e^{(1+a_3 y_{M,j})}(4\alpha T_{M-1,j} - \alpha T_{M-2,j} + \beta T_{M,j+1} - \beta T_{M,j-1}) + 2hJ\sqrt{\alpha}T_\infty}{3a_1 e^{(1+a_2 x_{M,j})} e^{(1+a_3 y_{M,j})}\alpha + 2hJ\sqrt{\alpha}} \tag{24}$$

In a similar fashion, we can compute the temperature distribution on the inner surface Γ_i. At the inner surface Γ_i, we have

$$\dot{q} = k\frac{\partial T}{\partial n_i} \tag{25}$$

$$\dot{q} = k\left(\frac{-1}{J\sqrt{\alpha}}(\alpha T_\xi - \beta T_\eta)\right) \tag{26}$$

where

$$T_\xi = \frac{1}{2}(-3T_{1,j} + 4T_{2,j} - T_{3,j}) \tag{27}$$

$$T_\eta = \frac{1}{2}(T_{1,j+1} - T_{1,j-1}) \tag{28}$$

Therefore, Eq. (19) becomes

$$\dot{q} = k_{1,j}\left[\frac{-1}{J\sqrt{\alpha}}\left(\alpha\frac{-3T_{1,j} + 4T_{2,j} - T_{3,j}}{2} - \beta\frac{T_{1,j+1} - T_{1,j-1}}{2}\right)\right] \tag{29}$$

where the coefficients J, α, and β are computed using the finite-difference coefficients associated with the inner surface Γ_i. Solving Eq. (22) for $T_{1,j}$ gives the temperature distribution on the boundary surface Γ_i as follows

$$T_{1,j} = \frac{k_{1,j}(4\alpha T_{2,j} - \alpha T_{3,j} - \beta T_{1,j+1} + \beta T_{1,j-1}) + 2\dot{q}J\sqrt{\alpha}}{3k_{1,j}\alpha} \tag{30}$$

or

$$T_{1,j} = \frac{a_1 e^{(1+a_2 x_{1,j})} e^{(1+a_3 y_{1,j})}(4\alpha T_{2,j} - \alpha T_{3,j} - \beta T_{1,j+1} + \beta T_{1,j-1}) + 2\dot{q}J\sqrt{\alpha}}{3a_1 e^{(1+a_2 x_{1,j})} e^{(1+a_3 y_{1,j})}\alpha} \tag{31}$$

Since the branch cut (*AB* or *CD* in Fig. 1a) is inside the physical domain, the same procedure employed to obtain an algebraic expression for $T_{i,j}$ (Eq. (14)) can also be used to obtain an expression for the temperature on the branch cut, $T_{i,1}$ (and hence $T_{i,N}$, as $T_{i,1} = T_{i,N}$, $i = 1,\ldots,M$). However, some changes are needed in the terms discretized by the finite-difference method (Equation (12)) as follows (Fig. 3)

$$f_\xi = \frac{1}{2}(f_{i+1,1} - f_{i-1,1})$$

$$f_\eta = \frac{1}{2}(f_{i,2} - f_{i,N-1})$$

$$f_{\xi\xi} = f_{i+1,1} - 2f_{i,1} + f_{i-1,1}$$

$$f_{\eta\eta} = f_{i,2} - 2f_{i,1} + f_{i,N-1}$$

$$f_{\xi\eta} = \frac{1}{4}(f_{i+1,2} - f_{i-1,2} - f_{i+1,N-1} + f_{i-1,N-1}) \tag{32}$$

where $f \equiv x, y, T$.

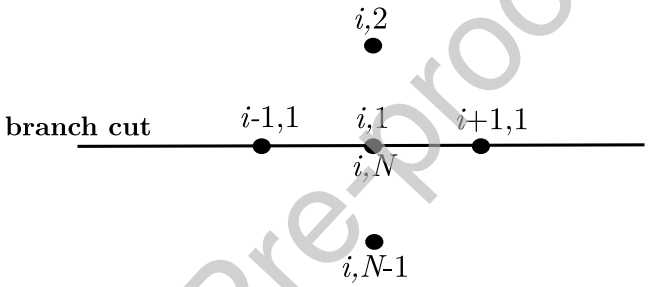

Fig. 3 Definition of nodes on the branch cut.

3. The inverse analysis

3.1 Objective function

The aim of this study is to simultaneously identify the heat flux applied at the inner surface Γ_i, $\dot{q}$, and the heat transfer coefficient at the outer surface Γ_o, h. To do so, an inverse analysis is used so that the square of the difference between the computed temperature of the outer surface Γ_o and the measured temperature of the same surface is minimized. This can be mathematically expressed as

$$\min \left\{ \underset{\dot{q} \text{ at } \Gamma_i, h \text{ at } \Gamma_o}{\mathsf{J}} := C \left\| T_{\Gamma_o} - T_m \right\|^2 : \text{Eq.(1) in } \Omega, \text{ BCs in Eqs.(2)-(3)} \right\} \tag{33}$$

where T_m is the measured temperature and C is a positive constant and can be considered as $C = 10^n, n = 0,1,2,\ldots$. The inverse analysis is used to minimize the following objective function expression:

$$\mathsf{J} = C\sum_{j=2}^{N-1}(T_{M,j} - T_{(M,j)_m})^2 \tag{34}$$

3.2 Sensitivity analysis

Computation of derivative of objective function with respect to unknown variables is required in gradient-based optimization methods. Here the inverse problem is concerned with the calculation of the sensitivity of the objective function J defined by Eq. (34) to $\dot{q}$ and h. Thus, we can write

$$\frac{\partial \mathsf{J}}{\partial h} = 2C\sum_{j=2}^{N-1}(T_{M,j} - T_{(M,j)_m})\frac{\partial T_{M,j}}{\partial h} = 2\sum_{j=2}^{N-1}(T_{M,j} - T_{(M,j)_m})C\frac{\partial T_{M,j}}{\partial h} \tag{35}$$

$$\frac{\partial \mathsf{J}}{\partial \dot{q}} = 2C\sum_{j=2}^{N-1}(T_{M,j} - T_{(M,j)_m})\frac{\partial T_{M,j}}{\partial \dot{q}} = 2\sum_{j=2}^{N-1}(T_{M,j} - T_{(M,j)_m})C\frac{\partial T_{M,j}}{\partial \dot{q}} \tag{36}$$

In Eqs. (35) and (36), $C\dfrac{\partial T_{M,j}}{\partial h}$ and $C\dfrac{\partial T_{M,j}}{\partial \dot{q}}$ are called the sensitivity coefficients and may be explicitly expressed by taking derivative of Eq. (23) with respect to the heat transfer coefficient h and the heat flux $\dot{q}$ as follows

$$\frac{\partial T_{M,j}}{\partial h} = \frac{2J\sqrt{\alpha}k_{M,j}(-4\alpha T_{M-1,j} + \alpha T_{M-2,j} - \beta T_{M,j+1} + \beta T_{M,j-1} + 3\alpha T_{\infty})}{(3k_{M,j}\alpha + 2hJ\sqrt{\alpha})^2} \tag{37}$$

For the exponentially varying thermal conductivity $k = a_1 e^{(1+a_2 x)} e^{(1+a_3 y)}$ we can write Eq. (37) as

$$\frac{\partial T_{M,j}}{\partial h} = \frac{2J\sqrt{\alpha}a_1 e^{(1+a_2 x_{M,j})} e^{(1+a_3 y_{M,j})}(-4\alpha T_{M-1,j} + \alpha T_{M-2,j} - \beta T_{M,j+1} + \beta T_{M,j-1} + 3\alpha T_{\infty})}{(3a_1 e^{(1+a_2 x_{M,j})} e^{(1+a_3 y_{M,j})}\alpha + 2hJ\sqrt{\alpha})^2} \tag{38}$$

As the heat flux $\dot{q}$ is applied at the inner surface and the temperature measurements are taken on the outer surface (a different surface from the applied heat flux surface), chain rule (using the thermal conductivity components such as a_2 or a_3) may be used to relate the simulated measured temperature $T_{M,j}$ to the heat flux $\dot{q}$ as follows

$$\frac{\partial T_{M,j}}{\partial \dot{q}} = \frac{\dfrac{\partial T_{M,j}}{\partial a_2}}{\dfrac{\partial \dot{q}}{\partial a_2}} \tag{39}$$

we can write Eq. (26), as follows

$$\dot{q} = k\left(\frac{-1}{J\sqrt{\alpha}}(\alpha T_{\xi} - \beta T_{\eta})\right)\Big|_{\Gamma_i} = a_1 e^{(1+a_2 x_{1,j})} e^{(1+a_3 y_{1,j})} \left(\frac{-1}{J\sqrt{\alpha}}(\alpha T_{\xi} - \beta T_{\eta})\right)\Big|_{\Gamma_i} \tag{40}$$

Hence, the denominator of Eq. (39) can be written as

$$\frac{\partial \dot{q}}{\partial a_2} = a_1 x_{1,j} e^{(1+a_2 x_{1,j})} e^{(1+a_3 y_{1,j})} \left(\frac{-1}{J\sqrt{\alpha}}(\alpha T_{\xi} - \beta T_{\eta})\right)\Big|_{\Gamma_i} \tag{41}$$

where the terms T_{ξ}, T_{η}, J, α, and β are computed using the finite-difference coefficients associated with the inner surface Γ_i (as in Eq. (29)). Moreover, the numerator of Eq. (39) can be obtained by taking derivative of $T_{M,j}$ with respect to a_2 using Eq. (24), as follows

$$\frac{\partial T_{M,j}}{\partial a_2} = \frac{2a_1 x_{M,j} e^{(1+a_2 x_{M,j})} e^{(1+a_3 y_{M,j})} hJ\sqrt{\alpha}(4\alpha T_{M-1,j} - \alpha T_{M-2,j} + \beta T_{M,j+1} - \beta T_{M,j-1} - 3\alpha T_{\infty})}{(3a_1 e^{(1+a_2 x_{M,j})} e^{(1+a_3 y_{M,j})}\alpha + 2hJ\sqrt{\alpha})^2} \tag{42}$$

Therefore, the expression in Eq. (39) can be computed by dividing the expression in Eq. (42) by the one in Eq. (41):

$$\frac{\partial T_{M,j}}{\partial \dot{q}} = \frac{2a_1 x_{M,j} e^{(1+a_2 x_{M,j})} e^{(1+a_3 y_{M,j})} hJ\sqrt{\alpha}(4\alpha T_{M-1,j} - \alpha T_{M-2,j} + \beta T_{M,j+1} - \beta T_{M,j-1} - 3\alpha T_{\infty})}{(3a_1 e^{(1+a_2 x_{M,j})} e^{(1+a_3 y_{M,j})}\alpha + 2hJ\sqrt{\alpha})^2 \left(a_1 x_{1,j} e^{(1+a_2 x_{1,j})} e^{(1+a_3 y_{1,j})} \left(\frac{-1}{J\sqrt{\alpha}}(\alpha T_{\xi} - \beta T_{\eta})\right)\Big|_{\Gamma_i}\right)} \tag{43}$$

Therefore, the sensitivity coefficients $C\dfrac{\partial T_{M,j}}{\partial h}$ and $C\dfrac{\partial T_{M,j}}{\partial \dot{q}}$ can be computed in only one single direct problem solution without the need for solving an adjoint equation. The sensitivity matrix $\mathbf{Ja}$ can be explicitly written as

$$\mathbf{Ja}_h = C\begin{bmatrix} \dfrac{\partial T_{M,2}}{\partial h} \\ \dfrac{\partial T_{M,3}}{\partial h} \\ \vdots \\ \dfrac{\partial T_{M,N-1}}{\partial h} \end{bmatrix}_{(N-2)\times 1} , \mathbf{Ja}_{\dot{q}} = C\begin{bmatrix} \dfrac{\partial T_{M,2}}{\partial \dot{q}} \\ \dfrac{\partial T_{M,3}}{\partial \dot{q}} \\ \vdots \\ \dfrac{\partial T_{M,N-1}}{\partial \dot{q}} \end{bmatrix}_{(N-2)\times 1} \tag{44}$$

3.3 The Conjugate Gradient Method (CGM)

The conjugate gradient optimization method (a gradient-based optimization method) is used here to solve the inverse heat transfer problem. The objective function given by Eq. (34) is minimized by searching along the direction of descent $d^{(\mathrm{k})}$ using a search step length $\beta^{(\mathrm{k})}$.

$$f^{(\mathrm{k}+1)} = f^{(\mathrm{k})} - \beta^{(\mathrm{k})} d^{(\mathrm{k})} \tag{45}$$

where $f \equiv h, \dot{q}$. The direction of descent of the current iteration is obtained as a linear combination of the direction of descent of the previous iteration and the gradient direction $\nabla \mathbf{J}^{(\mathrm{k})}$. Therefore,

$$d^{(\mathrm{k})} = \nabla \mathbf{J}^{(\mathrm{k})} + \gamma^{(\mathrm{k})} d^{(\mathrm{k}-1)} \tag{46}$$

The Polak-Ribiere formula [53] is used to compute the conjugation coefficient:

$$\gamma^{(\mathrm{k})} = \frac{\left[\nabla \mathbf{J}^{(\mathrm{k})}\right]^{\mathrm{T}} (\nabla \mathbf{J}^{(\mathrm{k})} - \nabla \mathbf{J}^{(\mathrm{k}-1)})}{\| \nabla \mathbf{J}^{(\mathrm{k}-1)} \|^2} = \frac{\left[\nabla \mathbf{J}^{(\mathrm{k})}\right]^{\mathrm{T}} (\nabla \mathbf{J}^{(\mathrm{k})} - \nabla \mathbf{J}^{(\mathrm{k}-1)})}{\left[\nabla \mathbf{J}^{(\mathrm{k}-1)}\right]^{\mathrm{T}} \nabla \mathbf{J}^{(\mathrm{k}-1)}} \tag{47}$$

The search step-length is given as follows [41]

$$\beta^{(\mathrm{k})} = \frac{[\mathbf{Ja}^{(\mathrm{k})} d^{(\mathrm{k})}]^{\mathrm{T}} [T_{M,j} - T_{(M,j)_m}]}{[\mathbf{Ja}^{(\mathrm{k})} d^{(\mathrm{k})}]^{\mathrm{T}} [\mathbf{Ja}^{(\mathrm{k})} d^{(\mathrm{k})}]} \tag{48}$$

3.3.1 Optimization algorithm

The following algorithm presents the direct and inverse analysis steps used to simultaneously determine the heat flux applied at the inner surface of a functionally graded eccentric hollow cylinder and the heat transfer coefficient at the outer surface of the cylinder:

1. Specify the physical domain, the boundary conditions, and the measured outer surface temperature.

2. Generate the boundary-fitted grid using the elliptic grid generation method.

3. Solve the direct problem of finding the temperature values at any grid points of the physical domain using an initial values for the heat flux and the heat transfer coefficient (initial guess for h and $\dot{q}$).

4. Using Eq. (34), compute the objective function ($\mathbf{J}^{(\mathrm{k})}$).

5. If value of the objective function obtained in step 4 is less than the specified stopping criterion, the optimization is finished. Otherwise, go to step 6.

6. Compute the sensitivity matrices $\mathbf{Ja}_h$ and $\mathbf{Ja}_{\dot{q}}$ from Eq. (44)

7. Compute the gradient directions $\nabla \mathbf{J}_h^{(\mathrm{k})}$ and $\nabla \mathbf{J}_{\dot{q}}^{(\mathrm{k})}$ from Eqs. (35) and (36), respectively.

8. Compute the conjugation coefficients $\gamma_h^{(\mathrm{k})}$ and $\gamma_{\dot{q}}^{(\mathrm{k})}$ from Eq. (47). For $\mathrm{k}=0$, set $\gamma^{(0)}=0$.

9. Compute the directions of descent $d_h^{(\mathrm{k})}$ and $d_{\dot{q}}^{(\mathrm{k})}$ from Eq. (46).

10. Compute the search step lengths $\beta_h^{(\mathrm{k})}$ and $\beta_{\dot{q}}^{(\mathrm{k})}$ from Eq. (48).

11. From Eq. (45), evaluate the new values for h and $\dot{q}$ separately, namely $h^{(\mathrm{k}+1)}$ and $\dot{q}^{(\mathrm{k}+1)}$.

12. Set the next iteration ($\mathrm{k}=\mathrm{k}+1$) and return to the step 2.

3.4 stopping criterion

Without measurement errors, the inverse problem can be terminated if

$$\mathbf{J}^{(\mathrm{k})} < \varepsilon \tag{49}$$

where ε is a small specified number. In this study, for the case of no measurement error, $\varepsilon = 10^{-5}$ and $\varepsilon = 10^{-6}$ (depending on the value of C). However, the measured temperatures will contain errors. In this case, the objective function value will not be zero at the end of the iterative process. As the computed temperatures approach the measured temperatures containing errors, during the minimization of the objective function (Eq. (34)), large oscillations may appear in the inverse problem solution resulting in an ill-posed character for the inverse problem. However, the conjugate gradient method may become well-posed if the *Discrepancy Principle* is used to terminate the iterative procedure. In the Discrepancy Principle, if the difference between computed and measured temperatures is of the order of

magnitude of the measurement errors, then the solution is assumed to be sufficiently accurate, that is,

$$\left|T_{\text{computed}} - T_{\text{measured}}\right| \approx \sigma \tag{50}$$

where σ is the standard deviation of the measurement errors, which is assumed constant in the present analysis. We can obtain the following value for ε by substituting Eq. (50) into Eq. (34) (objective function definition)

$$\varepsilon = C(N-2)\sigma^2 \tag{51}$$

Then the iterative procedure is terminated when the following criterion is satisfied

$$\mathbf{J}^{(\mathrm{k})} < \varepsilon \tag{52}$$

4. Results

Since the numerical procedure explained here is concerned with an irregular shape (eccentric hollow cylinder) with different boundary conditions, we first validate the results of the heat conduction equation solution with the ones from the finite element analysis software COMSOL due to its capability to define analytical expression for the spatially varying thermal conductivity easily. To do so, a grid independency study is initially carried out for the exponential material graduation using four different grid sizes of 40×30, 60×50, 100×80, and 200×150. In the grid size of $M\times N$, M and N are the number of nodes in the radial and angular directions, respectively. The numerical values of the coefficients involved are listed in Table 1:

Table 1 Data used for the heat conduction problem involving exponential material graduation.

$\dot{q}(\frac{\mathrm{W}}{\mathrm{m}^2})$	$k(\frac{\mathrm{W}}{\mathrm{m}.^{\circ}\mathrm{C}})$	$h(\frac{\mathrm{W}}{\mathrm{m}^2.^{\circ}\mathrm{C}})$	$T_{\infty}(^{\circ}\mathrm{C})$
1000	$10e^{(1+0.02x_{i,j})}e^{(1+0.05y_{i,j})}$	10	30

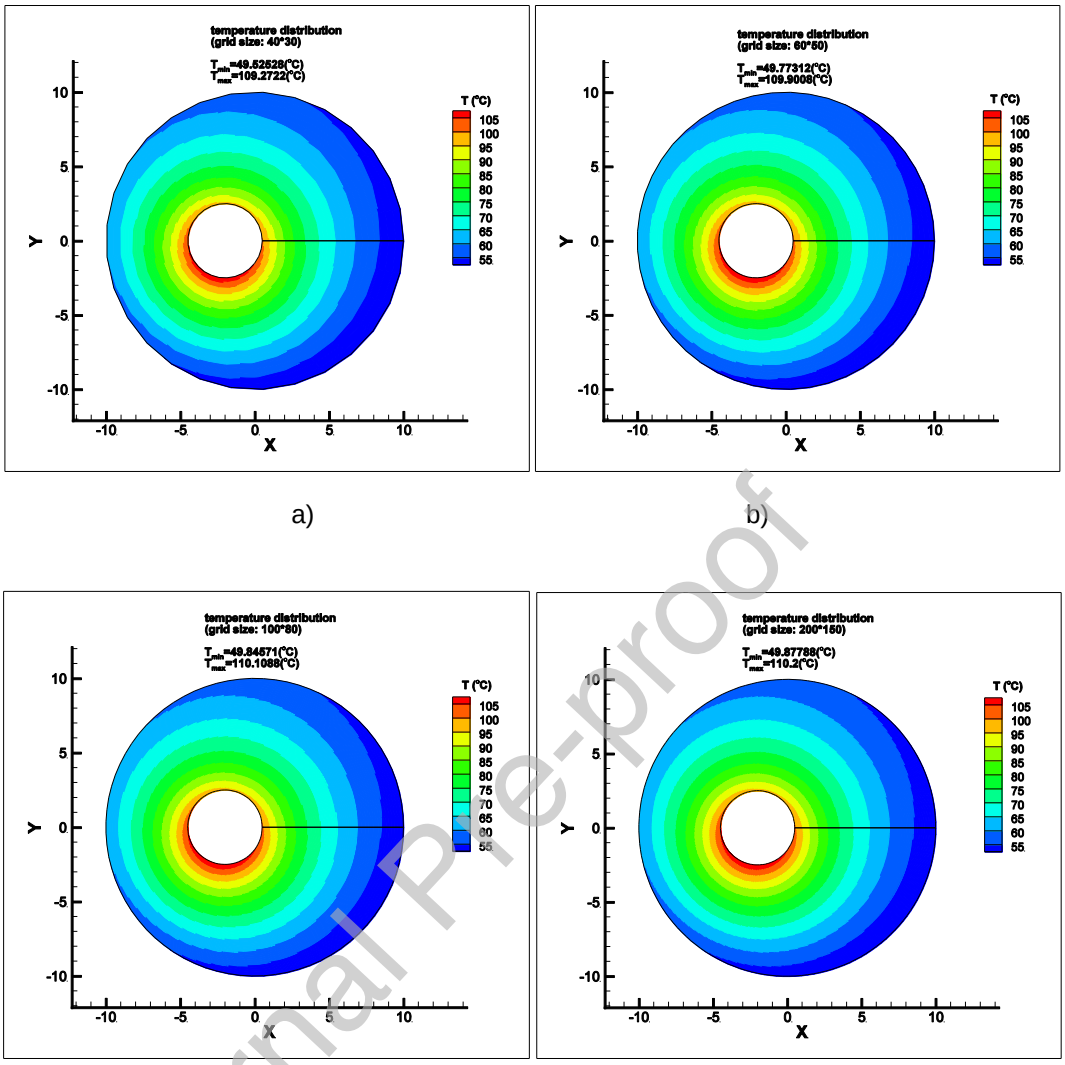

Fig. 4 Grid independency study of heat conduction equation solution for exponential material graduation. The temperature distribution using four different grid sizes of 40×30 (a), 60×50 (b), 100×80 (c), and 200×150 (d).

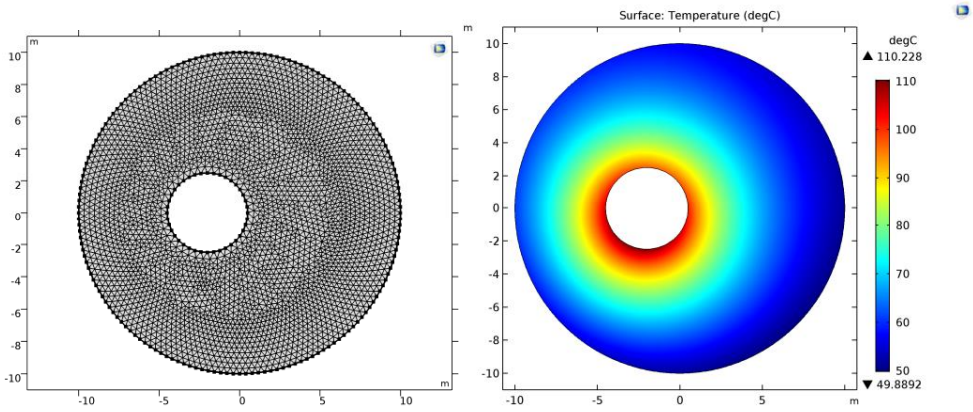

a) b)

Fig. 5 Solving the heat conduction equation using the finite element analysis solver COMSOL. The grid used (a) and the temperature distribution (b).

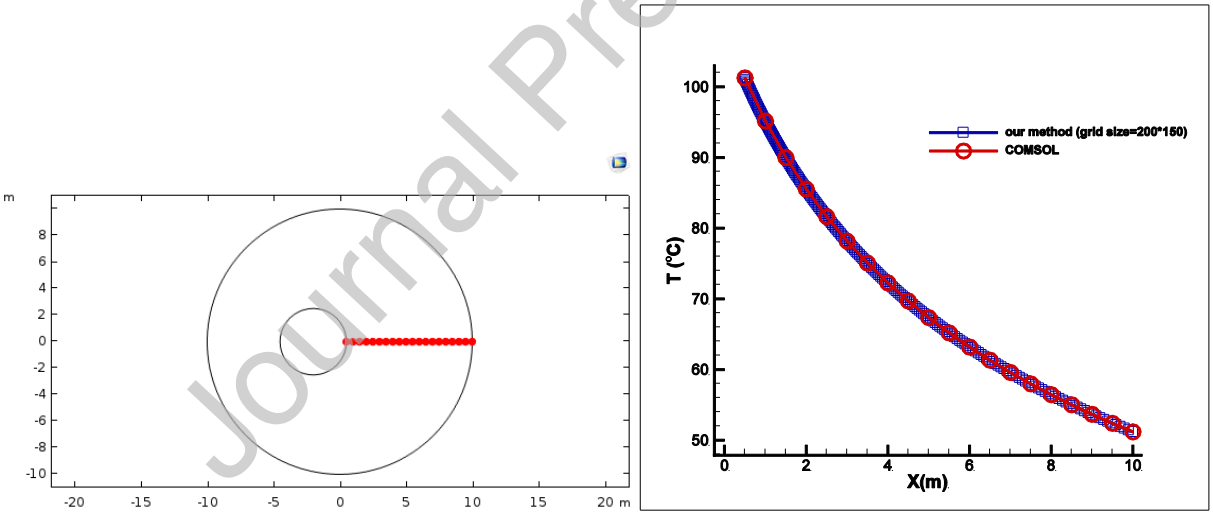

a) b)

Fig. 6 The comparison of temperatures obtained from the software COMSOL and our method. The points (20 points are used in COMSOL) on the branch cut (a) and the comparison of the temperatures on the branch cut (b).

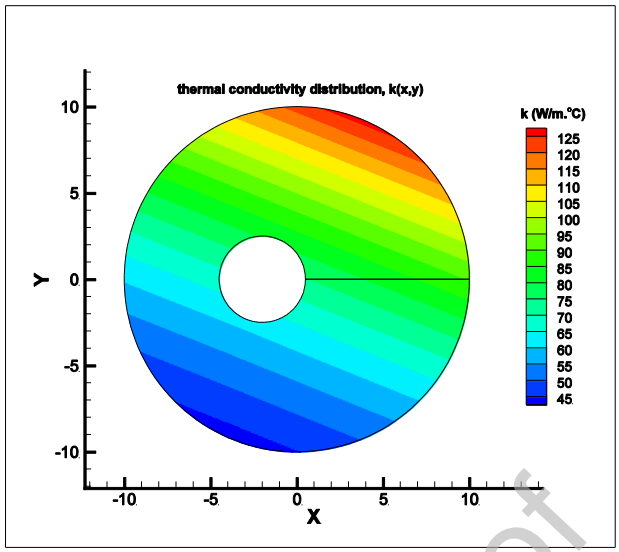

Fig. 7 Exponential graduation of thermal conductivity.

The result of the developed numerical method to solve heat conduction equation with the associated boundary conditions given in Table 1 is shown in Fig. 4 and the result from the solver COMSOL is depicted in Fig. 5. A comparison of the temperatures of the nodes on the branch cut (see Fig. 3) is depicted in Fig. 6. In this comparison the results obtained from the software COMSOL (using 20 points on the branch cut) and our code using the grid size of 200×150 is plotted. The comparison of the results from both numerical methods reveals an excellent agreement thereby confirming the correctness of the implementation and the accuracy of the proposed method. Moreover, the spatially varying thermal conductivity distribution over the body (FGM) is shown in Fig. 7.

Then the computed temperature distribution $T_{M,j}$ $(j=2,\ldots,N-1)$ is used as the *simulated* measured temperatures to recover the initially used heat flux and the heat transfer coefficient. In other words, the temperature distribution $T_{M,j}$ $(j=2,\ldots,N-1)$ obtained by solving the heat conduction equation using the numerical values specified in Table 1 is used to recover $\dot{q}=1000(\frac{\mathrm{W}}{\mathrm{m}^2})$ and $h=10(\frac{\mathrm{W}}{\mathrm{m}^2.^{\circ}\mathrm{C}})$. To facilitate the computation of the sensitivity matrix coefficients using the central finite-difference relations, the grid nodes $(M,1)$ and (M,N) on corners of the outer surface Γ_o are excluded from computing the temperature distribution. In the inverse analysis, the square of the difference between the temperature distribution of the outer surface Γ_o (obtained from the solution the direct problem at each iteration) and the simulated measured temperature distribution of the same surface (Γ_o) is to be minimized.

Test case: Using the problem data given in Table 1, the known (desired) values of $\dot{q}_d = 1000(\frac{\mathrm{W}}{\mathrm{m}^2})$ and $h_d = 10(\frac{\mathrm{W}}{\mathrm{m}^2.^\circ\mathrm{C}})$ are to be recovered by the proposed inverse analysis using the following three different initial guesses to demonstrate the robustness of the inverse analysis:

$$\dot{q}_{\text{initial}_1} = 500(\frac{\mathrm{W}}{\mathrm{m}^2}), h_{\text{initial}_1} = 2(\frac{\mathrm{W}}{\mathrm{m}^2.^\circ\mathrm{C}})$$

$$\dot{q}_{\text{initial}_2} = 2500(\frac{\mathrm{W}}{\mathrm{m}^2}), h_{\text{initial}_2} = 25(\frac{\mathrm{W}}{\mathrm{m}^2.^\circ\mathrm{C}})$$

$$\dot{q}_{\text{initial}_3} = 100(\frac{\mathrm{W}}{\mathrm{m}^2}), h_{\text{initial}_3} = 30(\frac{\mathrm{W}}{\mathrm{m}^2.^\circ\mathrm{C}})$$

Initial guess 1: $\dot{q}_{\text{initial}_1} = 500(\frac{\mathrm{W}}{\mathrm{m}^2}), h_{\text{initial}_1} = 2(\frac{\mathrm{W}}{\mathrm{m}^2.^\circ\mathrm{C}})$

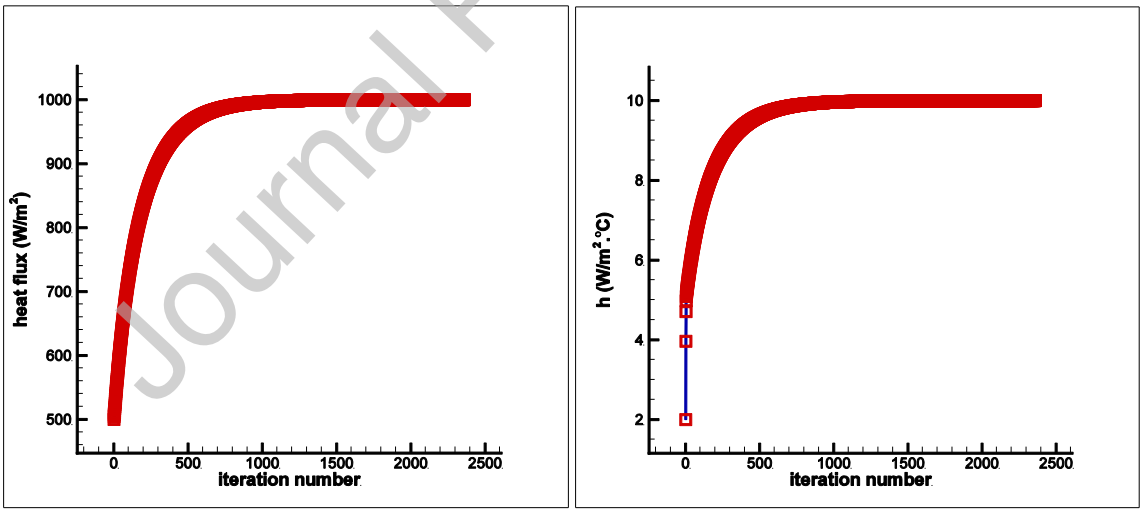

a) b)

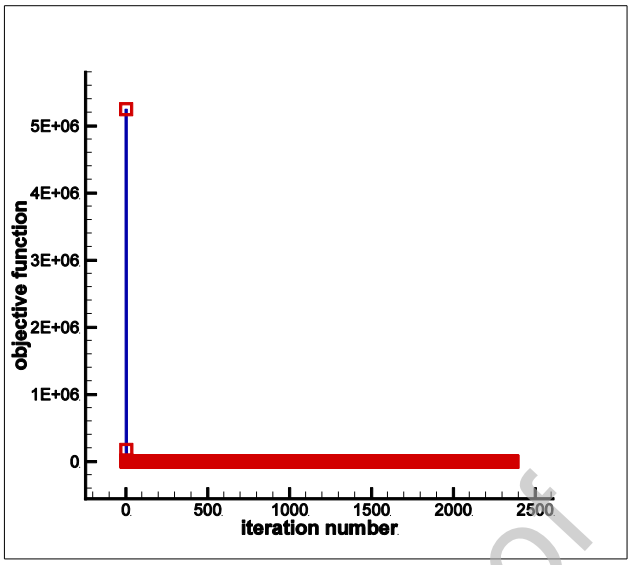

c)

Fig. 8 History of heat flux $\dot{q}$ (a), heat transfer coefficient h (b), and objective function for the initial guess $\dot{q}_{\text{initial}_1} = 500(\frac{\text{W}}{\text{m}^2}), h_{\text{initial}_1} = 2(\frac{\text{W}}{\text{m}^2.^\circ\text{C}})$ (c).

Initial guess 2: $\dot{q}_{\text{initial}_2} = 2500(\frac{\text{W}}{\text{m}^2}), h_{\text{initial}_2} = 25(\frac{\text{W}}{\text{m}^2.^\circ\text{C}})$

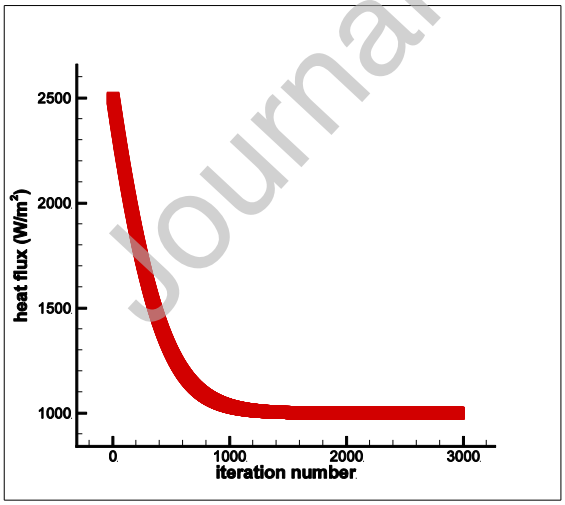

a)

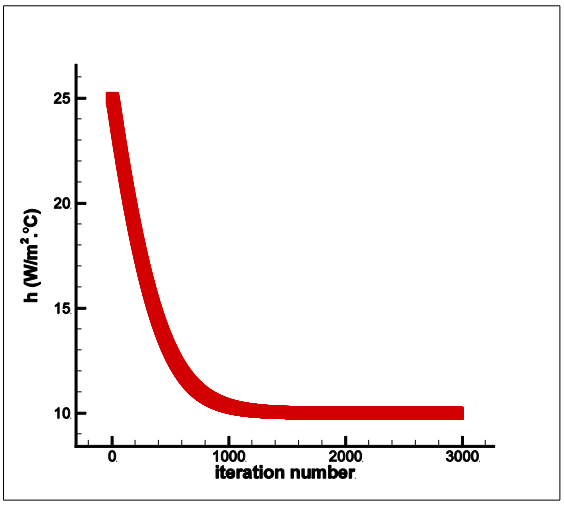

b)

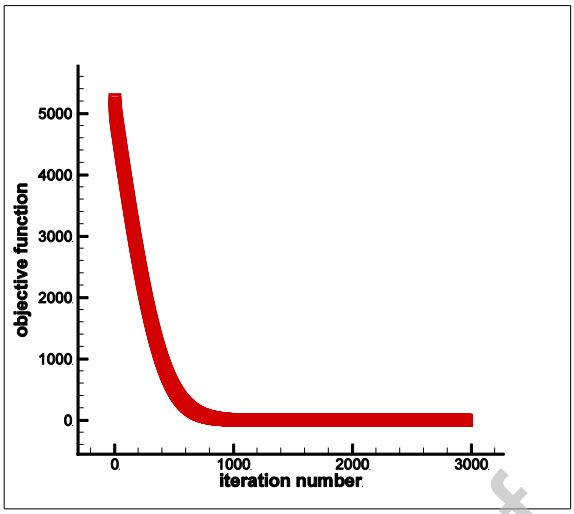

c)

Fig. 9 History of heat flux $\dot{q}$ (a), heat transfer coefficient h (b), and objective function for the initial guess $\dot{q}_{\text{initial}_2} = 2500(\frac{\text{W}}{\text{m}^2}), h_{\text{initial}_2} = 25(\frac{\text{W}}{\text{m}^2.^\circ\text{C}})$ (c).

Initial guess 3: $\dot{q}_{\text{initial}_3} = 100(\frac{\text{W}}{\text{m}^2}), h_{\text{initial}_3} = 30(\frac{\text{W}}{\text{m}^2.^\circ\text{C}})$

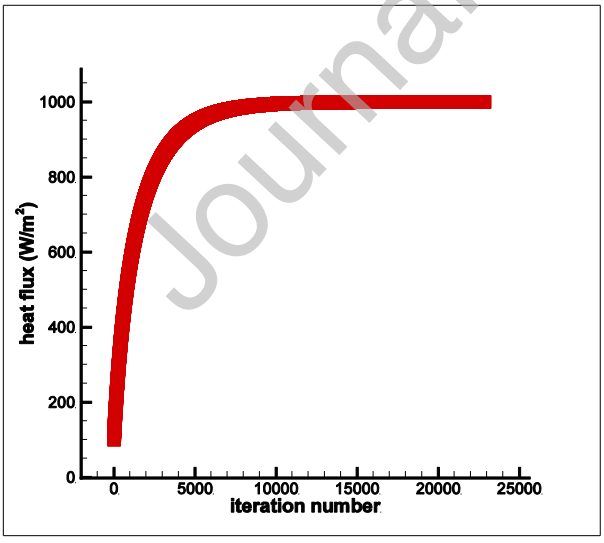

a)

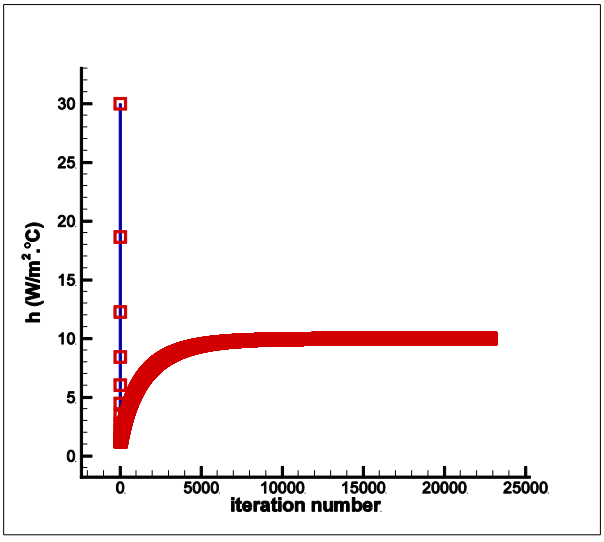

b)

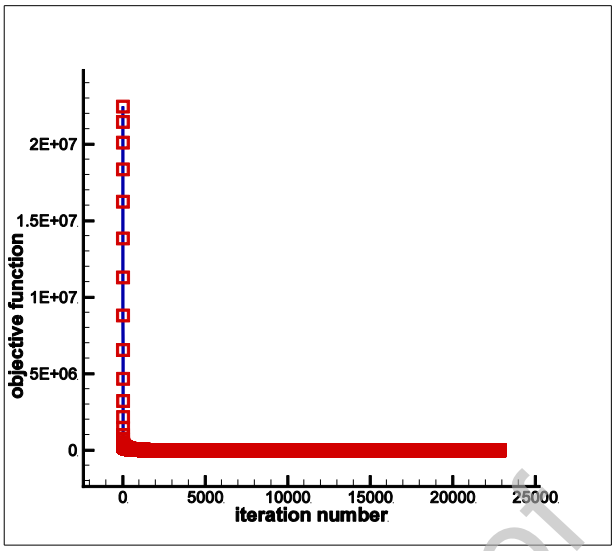

c)

Fig. 10 History of heat flux $\dot{q}$ (a), heat transfer coefficient h (b), and objective function for the initial guess $\dot{q}_{\text{initial}_3} = 100(\frac{\text{W}}{\text{m}^2}), h_{\text{initial}_3} = 30(\frac{\text{W}}{\text{m}^2.^\circ\text{C}})$ (c).

Initial guess 2 (with measurement error): $\dot{q}_{\text{initial}_2} = 2500(\frac{\text{W}}{\text{m}^2}), h_{\text{initial}_2} = 25(\frac{\text{W}}{\text{m}^2.^\circ\text{C}})$

In this study, the measured temperature containing random errors, $T_{M,j}^{\text{meas}}$ $(j = 2,\ldots,N-1)$, is generated by adding an error term $\omega\sigma$ to the exact temperature $T_{M,j}^{\text{exact}}$ to give

$$T_{M,j}^{\text{meas}} = T_{M,j}^{\text{exact}} + \omega\sigma \tag{53}$$

where ω is a random variable with normal distribution, zero mean, and unitary standard deviation. Assuming 99% confidence for the measured temperature, ω lies in the range $-2.576 \leq \omega \leq 2.576$ and it is randomly generated by using MATLAB. σ is the standard deviation of the measurement errors. In this study, $\sigma = 0.5$. The second initial guess, $\dot{q}_{\text{initial}_2} = 2500(\frac{\text{W}}{\text{m}^2}), h_{\text{initial}_2} = 25(\frac{\text{W}}{\text{m}^2.^\circ\text{C}})$ is considered to initiate the optimization process.

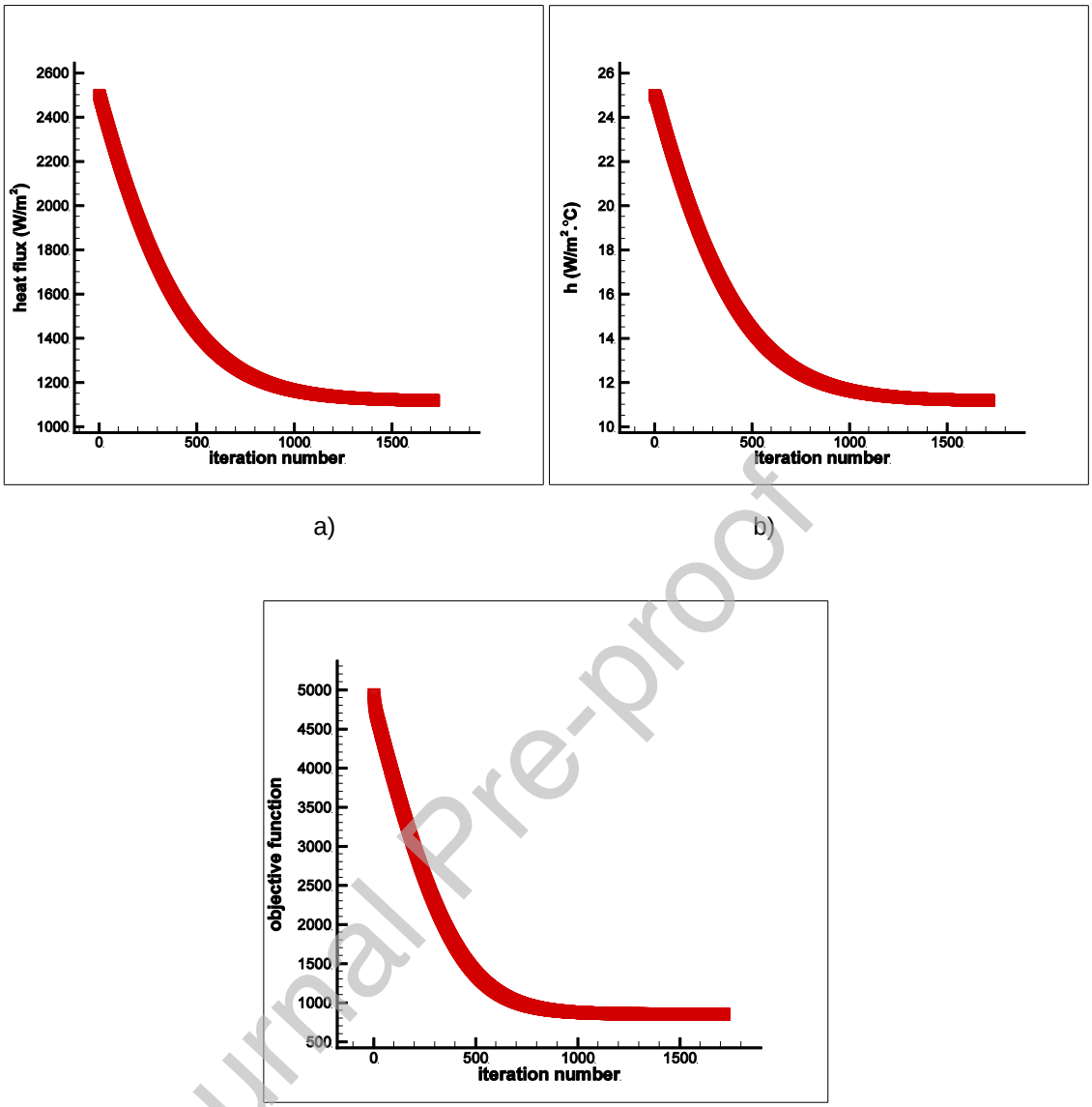

a) b)

c)

Fig. 11 History of heat flux $\dot{q}$ (a), heat transfer coefficient h (b), and objective function for the initial guess $\dot{q}_{\text{initial}_2} = 2500(\frac{\text{W}}{\text{m}^2}), h_{\text{initial}_2} = 25(\frac{\text{W}}{\text{m}^2.^\circ\text{C}})$ (c) by considering measurement error ($\sigma = 0.5$).

Three different initial guesses are used to analyze the inverse analysis presented here. The initial guesses are selected so that they can reflect the accuracy, efficiency, and robustness of the inverse analysis. The convergence histories of the heat flux and the heat transfer coefficient for all three initial guesses are depicted in Fig. 8a,b, Fig. 9a,b, Fig. 10a,b, and Fig. 11a,b (for the measurement error case), respectively. As shown in Fig. 8c, Fig. 9c, and Fig.

10c, a 100% reduction in the objective function and complete recovering of the values for $\dot{q}$ and h (the heat flux and the heat transfer coefficient, respectively) are achieved by starting the optimization process from the initial guesses which are numerically far from the desired ones thereby confirming the robustness of the developed numerical procedure. Despite the large number of iterations for recovering the unknown variables, short computation time reveals the efficiency of the developed method. The details of the results, including the initial and final values for $\dot{q}$ and h, the initial and final values of the objective function, the computation time, the number of iterations, and the percentage of the decrease in the objective function, are given in Table 2 (for both cases of no measurement error and a measurement error). In case of the measurement error ($\sigma = 0.5$), there is also a significant reduction (82.7%) in the objective function value (Fig. 11c). As shown in Table 2, for $\sigma = 0.5$ the errors in recovering the parameters h and $\dot{q}$ are 12% and 11.9%, respectively. The results are obtained by a FORTRAN compiler and computations are run on a PC with Intel Core i5 and 6G RAM. A tolerance of 10^{-7} is used in iterative loops to increase the accuracy of results.

Table 2 A summary of results for the simultaneous determination of the heat flux $\dot{q}$ and the heat transfer coefficient h.

Grid size	Desired value	Initial (guess) value	Final value	Temperature measurement error	Initial value of J	Minimum value of J	Reduction in objective function & computation time
50×40	$\dot{q}=1000.0(\frac{\mathrm{W}}{\mathrm{m}^2})$ $h=10.0(\frac{\mathrm{W}}{\mathrm{m}^2.^\circ\mathrm{C}})$	$\dot{q}=500.0(\frac{\mathrm{W}}{\mathrm{m}^2})$ $h=2.0(\frac{\mathrm{W}}{\mathrm{m}^2.^\circ\mathrm{C}})$	$\dot{q}=1000.0(\frac{\mathrm{W}}{\mathrm{m}^2})$ $h=10.0(\frac{\mathrm{W}}{\mathrm{m}^2.^\circ\mathrm{C}})$	$\sigma=0$	5249371.48 $(C=100)$	9.98×10^{-7} $(C=100)$	100% (31m:04s) (2360 iterations)
50×40	$\dot{q}=1000.0(\frac{\mathrm{W}}{\mathrm{m}^2})$ $h=10.0(\frac{\mathrm{W}}{\mathrm{m}^2.^\circ\mathrm{C}})$	$\dot{q}=2500.0(\frac{\mathrm{W}}{\mathrm{m}^2})$ $h=25.0(\frac{\mathrm{W}}{\mathrm{m}^2.^\circ\mathrm{C}})$	$\dot{q}=1000.0(\frac{\mathrm{W}}{\mathrm{m}^2})$ $h=10.0(\frac{\mathrm{W}}{\mathrm{m}^2.^\circ\mathrm{C}})$	$\sigma=0$	5226.19 $(C=100)$	9.99×10^{-7} $(C=100)$	100% (47m:02s) (2956 iterations)
50×40	$\dot{q}=1000.0(\frac{\mathrm{W}}{\mathrm{m}^2})$ $h=10.0(\frac{\mathrm{W}}{\mathrm{m}^2.^\circ\mathrm{C}})$	$\dot{q}=100.0(\frac{\mathrm{W}}{\mathrm{m}^2})$ $h=30.0(\frac{\mathrm{W}}{\mathrm{m}^2.^\circ\mathrm{C}})$	$\dot{q}=1000.0(\frac{\mathrm{W}}{\mathrm{m}^2})$ $h=10.0(\frac{\mathrm{W}}{\mathrm{m}^2.^\circ\mathrm{C}})$	$\sigma=0$	22463354.18 $(C=1000)$	9.99×10^{-6} $(C=1000)$	100% (111m) (22829 iterations)
50×40	$\dot{q}=1000.0(\frac{\mathrm{W}}{\mathrm{m}^2})$ $h=10.0(\frac{\mathrm{W}}{\mathrm{m}^2.^\circ\mathrm{C}})$	$\dot{q}=2500.0(\frac{\mathrm{W}}{\mathrm{m}^2})$ $h=25.0(\frac{\mathrm{W}}{\mathrm{m}^2.^\circ\mathrm{C}})$	$\dot{q}=1118.9(\frac{\mathrm{W}}{\mathrm{m}^2})$ $(\mathrm{error}=11.89\%)$ $h=11.2(\frac{\mathrm{W}}{\mathrm{m}^2.^\circ\mathrm{C}})$ $(\mathrm{error}=12\%)$	$\sigma=0.5$	4939.79 $(C=100)$	853.99 $(C=100)$	82.7% (1714 iterations)

5. Conclusion

By developing an efficient, accurate, robust, and easy to implement explicit sensitivity analysis scheme, we presented in this study an inverse analysis to simultaneously determine boundary conditions in a steady-state heat conduction problem in a functionally graded eccentric hollow cylinder. The boundary conditions of interest here, namely, the heat flux and the heat transfer coefficient, were imposed on two different parts of the cylinder boundary. The heat flux was applied on the inner surface of the cylinder and the heat transfer coefficient was imposed at the outer surface. The cylinder was made from a functionally graded material in which the thermal conductivity was exponentially a function of position in the cylinder. Although the proposed numerical inverse analysis is applicable to general irregular heat conducting bodies, the hollow cylinder was chosen to analyze due to the importance of such a geometry in heat transfer analysis. In order to solve the steady-state heat conduction equation, the two-dimensional irregular heat-conducting body (eccentric hollow cylinder) was transformed into a regular computational domain to perform all computations related to the direct and inverse heat conduction solution. The discretization of the physical domain was performed by the elliptic grid generation and the approximation of the derivatives of the field variable (temperature) at the grid nodes by algebraic ones was performed by using the finite-difference method, a method chosen for the simplicity and the ease of implementation. The novelty of the inverse analysis lies in proposing an accurate and efficient explicit sensitivity analysis scheme with an advantage that it is not involved with an adjoint equation and additional solution of direct problem if the finite-difference method is used to calculate the sensitivity coefficients, and all the sensitivity coefficients can be computed efficiently in only one direct problem solution, without the need for the solution of the adjoint equation (to compute the gradient of the objective function with respect to the variables). As the heat flux was applied at the inner surface of the hollow cylinder and the temperature measurements were taken on a different surface, the chain rule using the variable thermal conductivity components was used to obtain an explicit relation between the temperature on the outer surface and the heat flux applied on the inner surface. The conjugate gradient method was used to minimize the objective function and recover the desired parameters accurately. The accuracy, efficiency, and robustness of the proposed numerical procedure were demonstrated through presenting a test case with three different initial guesses. Moreover, the results revealed that the retrieved parameters were not too much affected by introduction of a significant measurement error.

Declaration of Competing Interest

The authors declare no conflict of interest.

Acknowledgement

This research was supported by funding from the European Union's Horizon 2020 research and innovation programme under the Marie Skłodowska-Curie grant agreement No 663830.

References

[1] E. Artyukhin, Reconstruction of the thermal conductivity coefficient from the solution of the nonlinear inverse problem, Journal of Engineering Physics and Thermophysics, 41(4) (1981) 1054-1058. https://doi.org/10.1007/BF00824761
[2] O.M. Alifanov, A.P. Tryanin, Determination of the coefficient of internal heat exchange and the effective thermal conductivity of a porous solid on the basis of a nonstationary experiment, Journal of Engineering Physics, 48(3) (1985) 356-365. https://doi.org/10.1007/BF00878206
[3] L. Dantas, H. Orlande, A function estimation approach for determining temperature-dependent thermophysical properties, Inverse Problems in Engineering, 3(4) (1996) 261-279. https://doi.org/10.1080/174159796088027627
[4] T. Jurkowski, Y. Jarny, D. Delaunay, Estimation of thermal conductivity of thermoplastics under moulding conditions: an apparatus and an inverse algorithm, International Journal of Heat and Mass Transfer, 40(17) (1997) 4169-4181. https://doi.org/10.1016/S0017-9310(97)00027-6
[5] C.-y. Yang, A linear inverse model for the temperature-dependent thermal conductivity determination in one-dimensional problems, Applied Mathematical Modelling, 22(1–2) (1998) 1-9. http://dx.doi.org/10.1016/S0307-904X(97)00101-7
[6] B. Sawaf, M.N. Ozisik, Y. Jarny, An inverse analysis to estimate linearly temperature dependent thermal conductivity components and heat capacity of an orthotropic medium, International Journal of Heat and Mass Transfer, 38(16) (1995) 3005-3010. http://dx.doi.org/10.1016/0017-9310(95)00044-A
[7] E. Divo, A.J. Kassab, J.S. Kapat, M.-K. Chyu, Retrieval of multidimensional heat transfer coefficient distributions using an inverse BEM-based regularized algorithm: numerical and experimental results, Engineering Analysis with Boundary Elements, 29(2) (2005) 150-160. http://dx.doi.org/10.1016/j.enganabound.2004.08.006
[8] J. Zhang, M.A. Delichatsios, Determination of the convective heat transfer coefficient in three-dimensional inverse heat conduction problems, Fire Safety Journal, 44(5) (2009) 681-690. http://dx.doi.org/10.1016/j.firesaf.2009.01.004
[9] W.-L. Chen, Y.-C. Yang, H.-L. Lee, Inverse problem in determining convection heat transfer coefficient of an annular fin, Energy Conversion and Management, 48(4) (2007) 1081-1088. http://dx.doi.org/10.1016/j.enconman.2006.10.016
[10] M. Mierzwiczak, J.A. Kołodziej, The determination temperature-dependent thermal conductivity as inverse steady heat conduction problem, International Journal of Heat and Mass Transfer, 54(4) (2011) 790-796. http://dx.doi.org/10.1016/j.ijheatmasstransfer.2010.10.024
[11] B. Czél, G. Gróf, Inverse identification of temperature-dependent thermal conductivity via genetic algorithm with cost function-based rearrangement of genes, International Journal of Heat and Mass Transfer, 55(15–16) (2012) 4254-4263. http://dx.doi.org/10.1016/j.ijheatmasstransfer.2012.03.067
[12] C.-H. Huang, Y. Jan-Yuan, An inverse problem in simultaneously measuring temperature-dependent thermal conductivity and heat capacity, International Journal of Heat

and Mass Transfer, 38(18) (1995) 3433-3441. http://dx.doi.org/10.1016/0017-9310(95)00059-I
[13] F. Mohebbi, M. Sellier, Parameter estimation in heat conduction using a two-dimensional inverse analysis, International Journal for Computational Methods in Engineering Science and Mechanics, 17(4) (2016) 274-287. https://doi.org/10.1080/15502287.2016.1204034
[14] F. Mohebbi, M. Sellier, T. Rabczuk, Estimation of linearly temperature-dependent thermal conductivity using an inverse analysis, International Journal of Thermal Sciences, 117 (2017) 68-76. https://doi.org/10.1016/j.ijthermalsci.2017.03.016
[15] F. Mohebbi, M. Sellier, Identification of space- and temperature-dependent heat transfer coefficient, International Journal of Thermal Sciences, 128 (2018) 28-37. https://doi.org/10.1016/j.ijthermalsci.2018.02.007
[16] F. Mohebbi, M. Sellier, Estimation of thermal conductivity, heat transfer coefficient, and heat flux using a three dimensional inverse analysis, International Journal of Thermal Sciences, 99 (2016) 258-270. https://doi.org/10.1016/j.ijthermalsci.2015.09.002
[17] P. Tervola, A method to determine the thermal conductivity from measured temperature profiles, International Journal of Heat and Mass Transfer, 32(8) (1989) 1425-1430. http://dx.doi.org/10.1016/0017-9310(89)90066-5
[18] S. Kim, A simple direct estimation of temperature-dependent thermal conductivity with kirchhoff transformation, International Communications in Heat and Mass Transfer, 28(4) (2001) 537-544. http://dx.doi.org/10.1016/S0735-1933(01)00257-3
[19] J.-H. Lin, C.-K. Chen, Y.-T. Yang, Inverse method for estimating thermal conductivity in one-dimensional heat conduction problems, Journal of Thermophysics and Heat Transfer, 15(1) (2001) 34-41. https://doi.org/10.2514/2.6593
[20] S. Chantasiriwan, Steady-state determination of temperature-dependent thermal conductivity, International Communications in Heat and Mass Transfer, 29(6) (2002) 811-819. http://dx.doi.org/10.1016/S0735-1933(02)00371-8
[21] B. Sawaf, M.N. Özisik, Determining the constant thermal conductivities of orthotropic materials by inverse analysis, International Communications in Heat and Mass Transfer, 22(2) (1995) 201-211. http://dx.doi.org/10.1016/0735-1933(95)00005-4
[22] T.T. Lam, W.K. Yeung, Inverse determination of thermal conductivity for one-dimensional problems, Journal of Thermophysics and Heat Transfer, 9(2) (1995) 335-344. https://doi.org/10.2514/3.665
[23] D. Lesnic, L. Elliott, D.B. Ingham, Identification of the thermal conductivity and heat capacity in unsteady nonlinear heat conduction problems using the boundary element method, Journal of Computational Physics, 126(2) (1996) 410-420. http://dx.doi.org/10.1006/jcph.1996.0146
[24] B. Konda Reddy, C. Balaji, Estimation of temperature dependent heat transfer coefficient in a vertical rectangular fin using liquid crystal thermography, International Journal of Heat and Mass Transfer, 55(13) (2012) 3686-3693. https://doi.org/10.1016/j.ijheatmasstransfer.2012.03.015
[25] H.R. Orlande, O. Fudym, D. Maillet, R.M. Cotta, Thermal measurements and inverse techniques, CRC Press, 2011.
[26] J. Taler, Determination of local heat transfer coefficient from the solution of the inverse heat conduction problem, Forschung im Ingenieurwesen, 71(2) (2007) 69-78. https://doi.org/10.1007/s10010-006-0044-2

[27] J. Taler, Nonlinear steady-state inverse heat conduction problem with space-variable boundary conditions, Journal of Heat Transfer (Transactions of the ASME (American Society of Mechanical Engineers), Series C);(United States), 114(4) (1992). https://doi.org/10.1115/1.2911877
[28] A.J. Kassab, E. Divo, A generalized boundary integral equation for isotropic heat conduction with spatially varying thermal conductivity, Engineering Analysis with Boundary Elements, 18(4) (1996) 273-286. https://doi.org/10.1016/S0955-7997(96)00057-4
[29] G. Flach, M. Özişik, Inverse heat conduction problem of simultaneously estimating spatially varying thermal conductivity and heat capacity per unit volume, Numerical Heat Transfer, 16(2) (1989) 249-266. https://doi.org/10.1080/10407788908944716
[30] S.R. Reddy, G.S. Dulikravich, S.J. Zeidi, Non-destructive estimation of spatially varying thermal conductivity in 3D objects using boundary thermal measurements, International Journal of Thermal Sciences, 118 (2017) 488-496. https://doi.org/10.1016/j.ijthermalsci.2017.05.011
[31] M.I.P. Hidayat, B.A. Wahjoedi, S. Parman, P.S.M. Yusoff, Meshless local B-spline-FD method and its application for 2D heat conduction problems with spatially varying thermal conductivity, Applied Mathematics and Computation, 242 (2014) 236-254. https://doi.org/10.1016/j.amc.2014.05.031
[32] J.V. Beck, Surface heat flux determination using an integral method, Nuclear Engineering and Design, 7(2) (1968) 170-178. https://doi.org/10.1016/0029-5493(68)90058-7
[33] C.H. Huang, S.P. Wang, A three-dimensional inverse heat conduction problem in estimating surface heat flux by conjugate gradient method, International Journal of Heat and Mass transfer, 42(18) (1999) 3387-3403. https://doi.org/10.1016/S0017-9310(99)00020-4
[34] F. Mohebbi, B. Evans, A. Shaw, M. Sellier, An inverse analysis for determination of space-dependent heat flux in heat conduction problems in the presence of variable thermal conductivity, International Journal for Computational Methods in Engineering Science and Mechanics, 20(3) (2019) 229-241. https://doi.org/10.1080/15502287.2019.1615579
[35] C.K. Hsieh, A.J. Kassab, A general method for the solution of inverse heat conduction problems with partially unknown system geometries, International Journal of Heat and Mass Transfer, 29(1) (1986) 47-58. https://doi.org/10.1016/0017-9310(86)90033-5
[36] F. Mohebbi, M. Sellier, Optimal shape design in heat transfer based on body-fitted grid generation, International Journal for Computational Methods in Engineering Science and Mechanics, 14(3) (2013) 227-243. https://doi.org/10.1080/15502287.2012.711426
[37] F. Mohebbi, M. Sellier, Three-dimensional optimal shape design in heat transfer based on body-fitted grid generation, International Journal for Computational Methods in Engineering Science and Mechanics, 14(6) (2013) 473-490. https://doi.org/10.1080/15502287.2013.784384
[38] F. Mohebbi, M. Sellier, T. Rabczuk, Inverse problem of simultaneously estimating the thermal conductivity and boundary shape, International Journal for Computational Methods in Engineering Science and Mechanics, (2017) 1-16. https://doi.org/10.1080/15502287.2017.1303006
[39] S.M.H. Sarvari, Optimal Geometry Design of Radiative Enclosures Using the Genetic Algorithm, Numerical Heat Transfer, Part A: Applications, 52(2) (2007) 127-143. https://doi.org/10.1080/10407780601115020
[40] O.M. Alifanov, Inverse heat transfer problems, Springer-Verlag, 1994.

[41] M. Özisik, H. Orlande, Inverse heat transfer: fundamentals and applications, Taylor & Francis, 2000.
[42] H.S. Shen, Functionally Graded Materials: Nonlinear Analysis of Plates and Shells, CRC Press, 2016.
[43] E.I. E, P. Demetris, G. Cristina, Mechanics Of Functionally Graded Material Structures, World Scientific Publishing Company, 2015.
[44] V. Birman, L.W. Byrd, Modeling and analysis of functionally graded materials and structures, Applied mechanics reviews, 60(5) (2007) 195-216. https://doi.org/10.1115/1.2777164
[45] J.N. Reddy, C.D. Chin, Thermomechanical analysis of functionally graded cylinders and plates, Journal of thermal stresses, 21(6) (1998) 593-626. https://doi.org/10.1080/01495739808956165
[46] M. Golbahar Haghighi, P. Malekzadeh, H. Rahideh, M. Vaghefi, Inverse transient heat conduction problems of a multilayered functionally graded cylinder, Numerical Heat Transfer, Part A: Applications, 61(9) (2012) 717-733. https://doi.org/10.1080/10407782.2012.671017
[47] W.-L. Chen, H.-M. Chou, Y.-C. Yang, An inverse problem in estimating the space-dependent thermal conductivity of a functionally graded hollow cylinder, Composites Part B: Engineering, 50 (2013) 112-119. https://doi.org/10.1016/j.compositesb.2013.02.010
[48] S.M. Hosseini, M. Akhlaghi, M. Shakeri, Transient heat conduction in functionally graded thick hollow cylinders by analytical method, Heat and Mass Transfer, 43(7) (2007) 669-675. https://doi.org/10.1007/s00231-006-0158-y
[49] W.-J. Chang, H.-L. Lee, Y.-C. Yang, Estimation of heat flux and thermal stresses in functionally graded hollow circular cylinders, Journal of thermal stresses, 34(7) (2011) 740-755. https://doi.org/10.1080/01495739.2010.550835
[50] E.M. Sparrow, M. Charmchi, Natural convection experiments in an enclosure between eccentric or concentric vertical cylinders of different height and diameter, International Journal of Heat and Mass Transfer, 26(1) (1983) 133-143. https://doi.org/10.1016/S0017-9310(83)80015-5
[51] T.H. Kuehn, R. Goldstein, An experimental study of natural convection heat transfer in concentric and eccentric horizontal cylindrical annuli, (1978). https://doi.org/10.1115/1.3450869
[52] F. Mohebbi, Optimal shape design based on body-fitted grid generation, University of Canterbury, (2014). http://hdl.handle.net/10092/9427
[53] E. Polak, G. Ribiere, Note sur la convergence de méthodes de directions conjuguées, Revue Française d'Informatique et de Recherche Opérationnelle, 16 (1969) 35–43. https://doi.org/10.1051/m2an/196903R100351